

## A MODIFIED ADAPTIVE GRID METHOD FOR RECIRCULATING FLOWS

D. LEE AND Y. M. TSUEI\*

*Institute of Aeronautics and Astronautics, National Cheng Kung University, Tainan, Taiwan, R.O.C. 700*

### SUMMARY

In this study a method of equidistribution of a weight function for grid adaption is modified to produce a smoother grid which yields a more accurate solution. In the original scheme the weight function was estimated on each grid independently and a large variation in the values of the weight function could generate a highly skewed and non-uniform grid which produced large errors. In this study the weight function is smoothed by coupling neighbouring weight functions. Abrupt changes in the weight function are alleviated and a smoother grid distribution is obtained. With relatively minor modifications of the original weight function it is demonstrated in this study that the solution can be improved. The test cases presented are the one-dimensional convection-diffusion equation, a laminar polar cavity flow, a laminar backward-facing step flow and a turbulent reacting sudden expansion pipe flow. Numerical efficiencies ranging from factors of five to 10 are achieved over uniform grid methods.

KEY WORDS Adaptive grid Truncation error Recirculating flows

### 1. INTRODUCTION

It is well known that fluid flows contain a wide range of length scales. Thin layers such as boundary layers, shock waves and flame fronts occur in many flows. Resolution of these regions is obviously essential to an accurate overall solution. To obtain an appropriate resolution, grids should be dense enough in the regions where needed to catch the fast variation of the flow characteristics. On the other hand, grids should be coarse in other regions to save both CPU time and computer storage. The problem is that the locations of the regions which require dense grids are not known *a priori* and therefore the grid must be adjusted as the solution proceeds. This technique is called the adaptive grid method. There are two approaches for grid adaption.<sup>1</sup> One is the global grid moving method<sup>2-5</sup> which uses a fixed number of grid points and lets them move to the region which requires a denser grid. A major concern in using this approach is the adequacy of the formulation of weight functions. The other approach is the local mesh refinement method<sup>6,7</sup> which adds and deletes grid points during the course of computation. The difficulty of this approach is primarily due to the required manipulation of data structures.

To adapt a grid, there must be a means of determining the regions where a denser grid is needed. Various strategies have been devised to serve this purpose. One strategy is to determine where large derivatives occur and another is to determine where large errors occur. Hedstrom and Rodrique<sup>8</sup> commented that the grid should be fine in the regions where the local truncation errors

---

\* Current address: Chung-Shan Institute of Science and Technology, Taiwan.

are large, not in the regions where derivatives of flow properties are large. Nevertheless, they also mentioned that in many cases derivatives of flow properties are pretty good error indicators. In a recent study<sup>9</sup> we showed that the truncation error of the convection terms in a curvilinear co-ordinate system is a function of the metric coefficients and flow property derivatives. Metric coefficients prescribe the grid configuration relative to a uniform one and flow property derivatives represent the changes of flow properties in the domain. A combination of these two factors determines the truncation error. This implies that large flow derivatives may yield large truncation errors. In other words, a proper resolution of high-gradient regions may improve the solution in many cases. The statement of Hedstrom and Rodrique that flow derivatives can be good error estimators is therefore not unfounded. Generally, for a complex physical problem it is difficult to estimate the truncation error directly and accurately. Therefore many researchers have employed the derivatives of the flow properties to construct the weight function for grid adaption. In addition, it is found in our study that, owing to inaccuracy and wide variation of the values of the truncation error, a stable grid cannot always be obtained. On the other hand, the moving grid method based on a flow property gradient distribution produces a more stable adaptive grid and yields an accuracy improvement. These facts show that, theoretically, the truncation error should be an ultimate measure of where an adaptive grid scheme should place points. In practice, using the truncation error to construct the weight function for grid adaption may not be a reliable method.

In the present study the moving grid method originally employed by Dwyer and co-workers<sup>2,3</sup> is modified by including a coupling between weight function values on neighbouring grid points. This modification implicitly smooths the distribution of the weight function and avoids discontinuities in the weight function. It is shown that with this minor modification to the weight function, grid quality as well as solution accuracy can be improved. This modified method is tested for the one-dimensional convection-diffusion equations, a two-dimensional laminar cavity flow, a backward-facing step flow and a turbulent reacting flow. The usefulness of the method is demonstrated.

## 2. MODIFIED MOVING GRID METHOD

Many of the moving grid methods fall into one of three categories:<sup>10,11</sup> the variational method, the equidistribution method and the grid speed method. Dwyer and co-workers<sup>2,3</sup> employed the concept of equidistributing weight functions  $W(s)$ . The mathematical expression for grid adaption in this technique is

$$\frac{\xi}{\xi_{\max}} = \frac{\int_0^s w ds}{\int_0^{s_{\max}} w ds}, \quad (1)$$

where  $\xi$  is one of the general co-ordinates in the transformed plane and  $s$  is the arc length along the  $\xi$ -line. If  $\xi$  is incremented with a constant value, equation (1) also implies

$$W_i \Delta s_i = \text{constant}. \quad (2)$$

If  $W_i$  is large,  $\Delta s_i$  becomes small and vice versa. Thus more grid points cluster in regions where  $W_i$  are large. The weight function  $W$  may have different forms depending on the characteristics of the physical problem. Dwyer<sup>3</sup> assumed the form

$$W(s) = 1 + \sum_i b_i \left| \frac{\partial \phi_i}{\partial s} \right|, \quad (3)$$

where the  $\phi_i$  are the relevant dependent variables considered in the grid adaption and the  $b_i$  are the 'normalizing factors' whose values are determined by the preassigned values of the parameters  $R_i$ ,

$$R_i = b_i \int_0^{s_{\max}} \left| \frac{\partial \phi_i}{\partial s} \right| ds \bigg/ \int_0^{s_{\max}} W ds. \quad (4)$$

The parameter  $R_i$ , which is between zero and unity, represents the fraction of the total number of grid points which will be allocated to the large-gradient regions of  $\phi_i$ . If the resolution of a variable  $\phi_i$  is important in a problem, a larger value of  $R_i$  may be assigned to that term. A more detailed account has been given in a previous study.<sup>12</sup> Note that the second-derivative terms used by Dwyer are eliminated from equation (3) in the present study. The inclusion of the higher-order derivative terms sometimes causes severe oscillation of the grid position in the course of adaption.<sup>12</sup>

Basically, the equidistribution scheme is a special case of the variational method in that only the volume measure  $I_v$ , using the notation in Reference 11, is minimized for grid adaption. Smoothness and orthogonality of the grid have not been taken into account in the scheme. As discussed in References 9, 13 and 14 as well as in the following section, truncation errors may increase significantly if grid size ratios are large. A sudden change of grid size in grid adaption is due to a sudden change of the weight function according to equation (2). To prevent such sudden changes in weight function values, one may either smooth the solution<sup>11</sup> or the weight function itself.<sup>15</sup> These smoothing treatments can be found, for example, in the work of Rai and Anderson,<sup>16,17</sup> who used a gravitational analogy for the moving grid wherein the grid points attract or repel each other. Special treatment for excessive stretching is needed in their method. Nakahashi and Deiwert<sup>18</sup> employed tension and torsion spring analogies to control the grid motion. In the present study, smoothing of the weight function  $W$  can be achieved implicitly by coupling the weight functions of neighbouring grid points. The modification is relatively simple and straightforward and can be conveniently extended to multidimensional flow problems. The computational overhead is minor.

In the formulation, the influence of the neighbouring weight function values on the grid  $(i, j)$  is arbitrarily assumed to decay exponentially with distance away from grid point  $(i, j)$ , then in a two-dimensional problem, along the  $\xi$ -lines, the weight function  $W_{ij}$  takes the form

$$W_{i,j} = 1 + \sum_N b_N \left( (\phi_\xi)_{i,j} + \sum_{\substack{k=1 \\ k \neq i}}^n (\phi_\xi)_{k,j} C_1 \exp(-|i-k|) + \sum_{\substack{l=1 \\ l \neq j}}^m (\phi_\xi)_{i,l} C_1 \exp(-|j-l|) \right)_N, \quad (5)$$

where  $N$  is the number of relevant variables considered,  $n$  and  $m$  are the numbers of points in the grid along the  $\xi$ - and the  $\eta$ -directions respectively,  $\phi_\xi$  is the derivative of the variable  $\phi$  and  $C_1$  is the coupling factor; if  $C_1 = 0$ , equation (5) reduces to equation (3). Note that the coupling used in the expression actually provides a means of smoothing the weight functions and a partial control over the skewness of the grid. Therefore no special treatment for excessive grid stretching or compression is required since it has been taken care of in the weight function formulation.

### 3. ADAPTIVE SOLUTIONS OF THE ONE-DIMENSIONAL MODEL EQUATION

In this section one-dimensional model equations are studied. The effect of coupling of the weight functions on the solutions is discussed. The usefulness and characteristics of the present modified moving grid method are demonstrated.

### 3.1. Convection–diffusion equation without source term

The one-dimensional convection–diffusion equation

$$u\phi_x = v\phi_{xx}, \quad (6)$$

with boundary conditions

$$\phi(0) = 0, \quad \phi(L) = 1,$$

has the exact solution

$$\phi(x) = \frac{e^{ux/v} - 1}{e^{uL/v} - 1}, \quad (7)$$

where  $u$  and  $v$  are constants and  $L$  is the overall length. By using the second-order central scheme and defining the grid size ratio  $r$  as

$$r = \frac{x_i - x_{i-1}}{x_{i+1} - x_i}, \quad (8)$$

the truncation error of the first-derivative term can be expressed as

$$T_E = -\frac{1}{2}\phi_{xx}(1-r)\Delta x - \frac{1}{6}\phi_{xxx}(1-r+r^2)\Delta x^2 + \text{higher-order terms}. \quad (9)$$

If a uniform grid is used, the local truncation error will be second-order and the accumulated leading truncation error can be estimated as

$$\begin{aligned} \varepsilon_{\text{uniform}} &= \int_0^L \frac{1}{6} \phi_{xxx} \left( \frac{L}{N} \right)^2 dx \\ &= \frac{1}{6} \left( \frac{1}{N} \right)^2 (Pe)^2, \end{aligned} \quad (10)$$

where  $N$  is the number of grid intervals and  $Pe$  is the overall grid Peclet number ( $=uL/v$ ). The accumulated truncation error is proportional to the square of the Peclet number and the square of the grid size. For an adaptive grid system, let the weight function take the form  $W = \phi_x$ . It may be shown that the grid size ratio  $r$  then becomes

$$r = e^{Pe_x}, \quad (11)$$

where  $Pe_x$  is the local Peclet number based on the mesh spacing. Note that  $r$  in this case is always greater than unity. If  $W$  takes the form of equation (3), i.e.  $W = 1 + b_1\phi_x$ ,  $r$  becomes

$$r = \frac{NPe_x + [(u/v)(L + b_1) - NPe_x]e^{Pe_x}}{(u/v)(L + b_1)}. \quad (12)$$

For the case of  $Pe = 50$  and  $N = 99$  the distributions of grid size ratio according to equations (11) and (12) are plotted in Figure 1. It is seen that in the first case  $r$  reaches the value of 67 and nearly all of the points are clustered near the end zone. On the other hand, adding '1' to the weight function expression leads to a much more reasonable grid size ratio distribution. Figure 2 shows that inadequate grid distribution induces higher error. The adaption with equation (12) reduces the error by an order of magnitude over the uniform grid solution. Note that in this figure the truncation error is plotted on a logarithmic scale. Figure 3 demonstrates that the grid distribution with equation (11) reduces the accuracy to first-order. The drawback of excessive stretching of the grid is obvious.

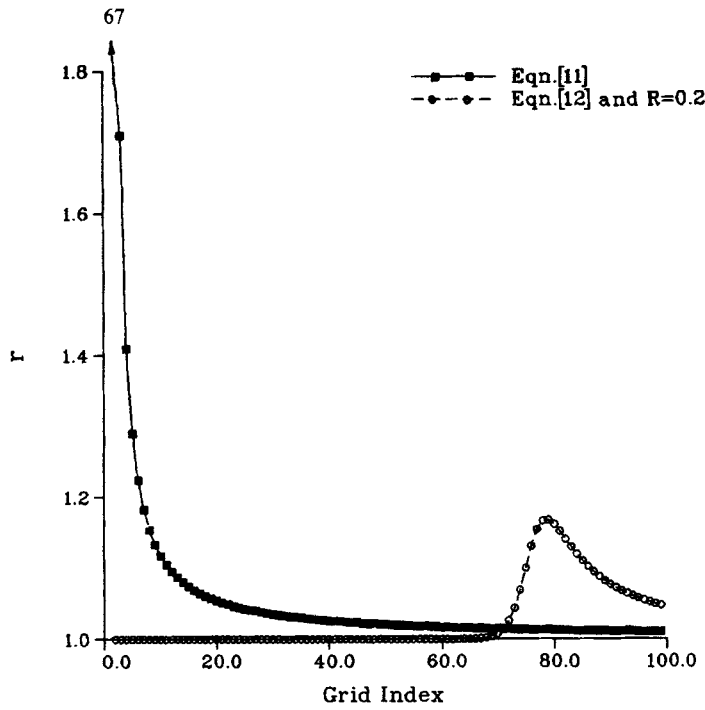


Figure 1. Distributions of grid size ratio using different weight functions

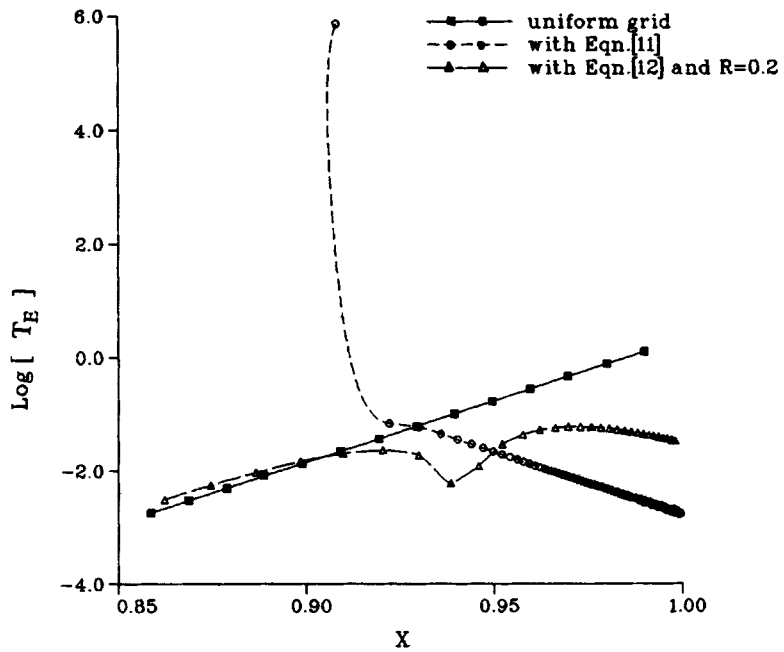


Figure 2. Error distributions for various grid arrangements

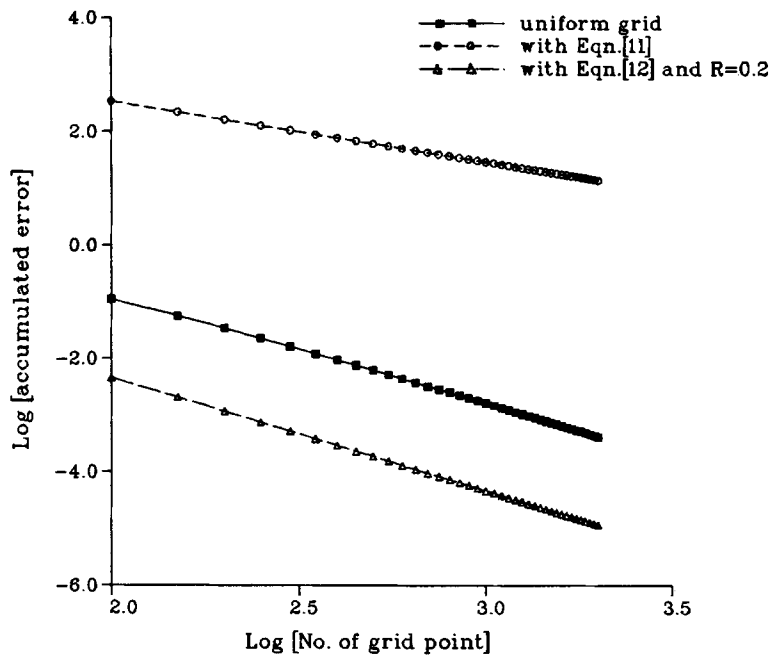


Figure 3. Error versus number of grid points

As mentioned before,  $R$  in equation (4) represents the percentage of the total grid which is allocated to the regions where a specific term in the weight function is important. If  $R$  is too small, grid adaption may not be effective. On the other hand, if  $R$  is too large, overstretching of the grid may occur. The problem is how to choose an appropriate  $R$ -value. In a previous study<sup>12</sup> the authors had some comments on the choice of  $R$ . In this study it is further confirmed that in general the optimum  $R$  will be between 0.1 and 0.3 in most cases. In the rest of this study  $R=0.2$  is selected unless otherwise specified. For the present test problem Figure 4 shows the error versus  $R$ -value for the case with  $Pe=50$ . It demonstrates that the moving grid method will be useful except if  $R$  is either too close to zero (uniform grid) or unity (excessive grid stretching). The method is most effective when the value is around 0.5.

Coupling of the weight functions can significantly reduce the maximum  $r$ -value and therefore the solution can generally be improved. The weight function in the present one-dimensional case takes the form

$$W_i = 1 + (\phi_x)_i + \sum_{\substack{k=1 \\ k \neq i}}^N (\phi_x)_k C_i \exp(-|i-k|). \quad (13)$$

Figure 5 compares the  $r$ -values of the coupled ( $C_i=1$ ) and uncoupled weight functions ( $C_i=0$ ). The maximum value of  $r$  is significantly reduced with the coupled weight function. Figure 6 depicts the solution using the modified method, which mimics the exact solution closely. Note that even with 500 grid points the adaptive solution with the uncoupled weight function still cannot capture the 'boundary layer' of the solution. This is due to an inadequate grid distribution. This inadequate grid is primarily due to an inadequate distribution of the weight function. Large grid size as well as large grid size ratio  $r$  near the boundary layer region are observed in this case ( $C_i=0$ , Figure 5). Consequently, the original scheme cannot adequately resolve the boundary

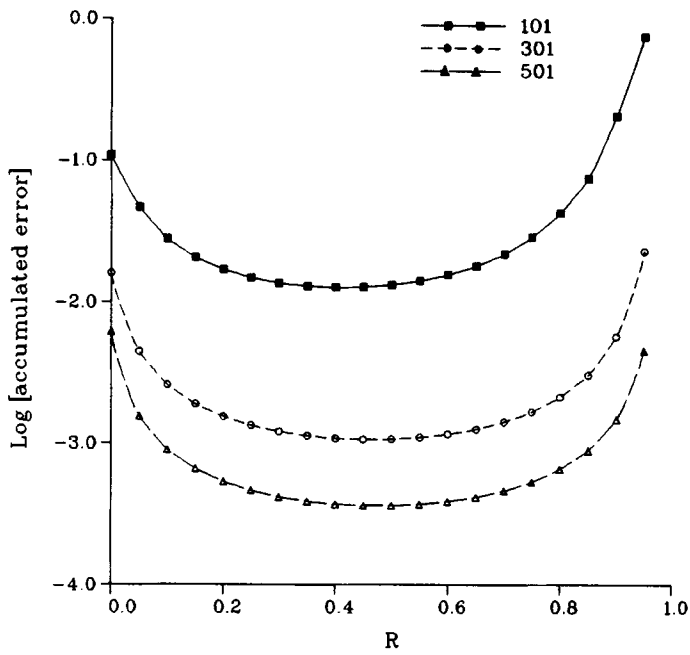


Figure 4. Error versus  $R$ ;  $Pe = 50$

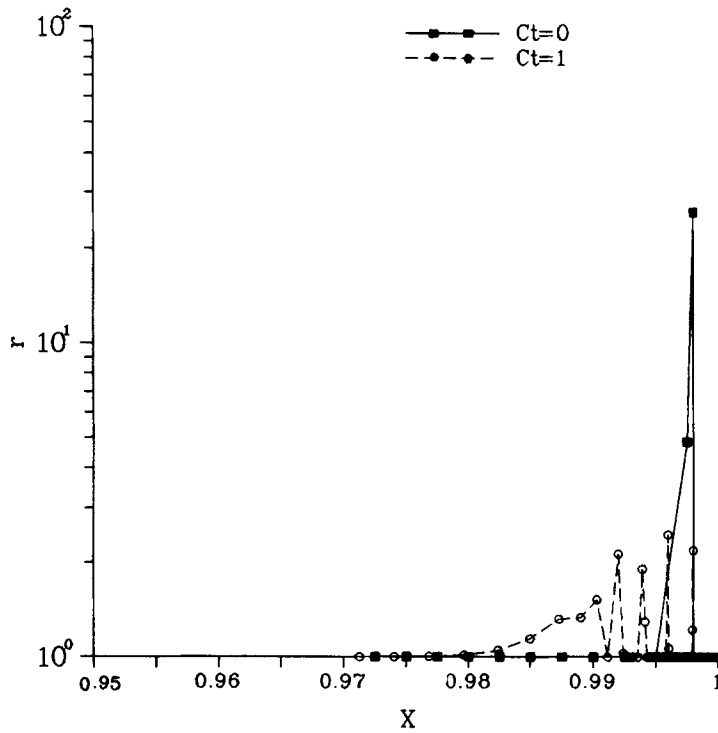


Figure 5. Distributions of grid size ratio using coupled and uncoupled weight functions;  $Pe = 1000$ ,  $N = 500$ ,  $R = 0.2$

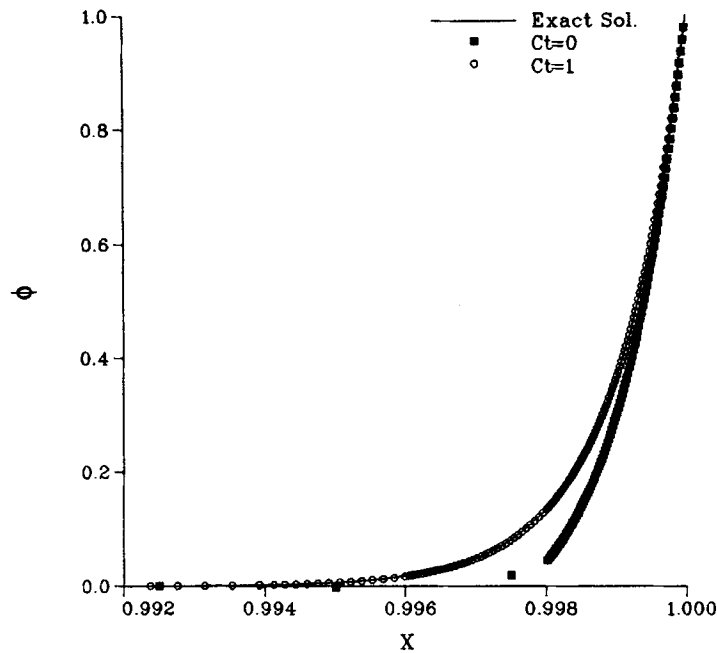


Figure 6. Improvement in adaptive solution using modified method;  $Pe = 1000$ ,  $N = 500$

layer region. On the other hand, the modified method provides a smoother grid distribution which properly resolves the region.

### 3.2. Convection-diffusion equation with source term

In this case the equation is

$$u\phi_x = v\phi_{xx} + S(x), \quad (14)$$

$$S(x) = \begin{cases} ax + b, & 0 \leq x < x_1, \\ \frac{ax_1 + b}{x_2} (x_1 + x_2 - x), & x_1 \leq x < x_1 + x_2, \\ 0, & x_1 + x_2 \leq x \leq L, \end{cases}$$

with boundary condition

$$\phi(0) = 0, \quad \phi(L) = 0,$$

where  $a = -2$ ,  $b = 3$ ,  $x_1 = 2h$ ,  $x_2 = h$ ,  $h = \frac{15}{16}$  and  $L = 15$ .

In this problem  $Pe = 1000$  and the grid number used is 501. On the choice of free parameter  $R$  it is found that the trend of the variation of error versus  $R$  is similar to the previous case. The optimal  $R$  is around 0.2. Again, coupling of the weight function improves the solution in the boundary layer region as shown in Figure 7. The original scheme ( $C_1 = 0$ ) yields a better solution than the uniform grid. However, it is still quite far from the exact one. The reason is similar to that discussed in the last problem. The solution using the modified method captures the exact solution almost perfectly.



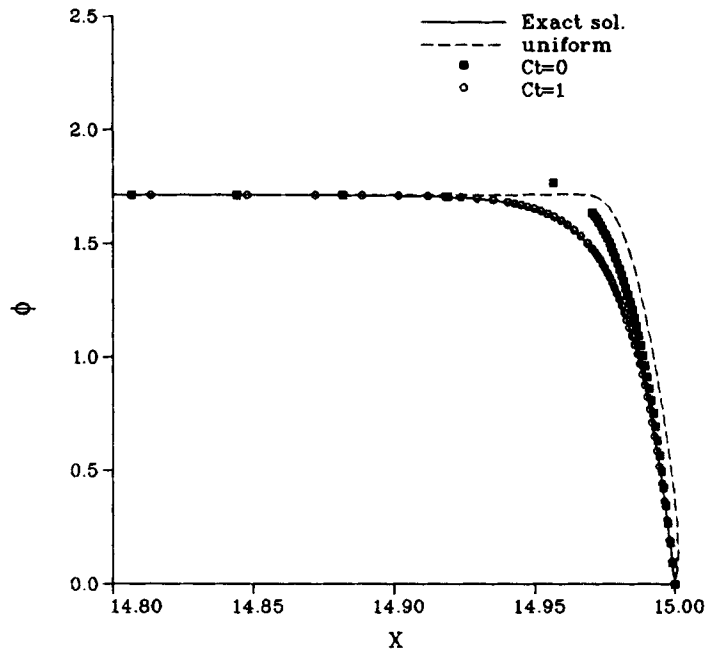


Figure 7. Solution improvement using modified method

#### 4. TWO-DIMENSIONAL FLOWS

In this section the modified moving grid method is applied to the computation of two-dimensional flows. The test problems chosen are a laminar polar cavity flow, a backward-facing step flow and a turbulent reacting sudden expansion pipe flow. Note that the convection terms are differenced by the second-order upwind scheme. Comparisons are made with the available experimental data for all three problems.

##### 4.1. Polar cavity flow

In this problem a laminar polar cavity flow with a sliding top at a Reynolds number of 350 is computed. Fuchs and Tillmark<sup>19</sup> studied this problem both experimentally and numerically. They obtained good agreement between the numerical results with  $80 \times 80$  meshes and their experimental data for this flow. Comparing our numerical solution for an  $81 \times 81$  uniform grid with their experimental data, it was found that good agreement was also obtained.<sup>20</sup> In the present study an even finer uniform grid solution,  $129 \times 129$ , is used as a reference solution for comparisons. The base grid in this test case is  $25 \times 25$ . In Figure 8 the adaptive grids with the coupled and uncoupled weight functions are depicted. Careful observation of this figure reveals that a better grid is obtained, in the sense that less acute angles and smoother grid size distribution are achieved, with the coupled weight function. The solution error distribution of the radial velocity component is shown in Figure 9. It is seen that the modified method ( $C_1 = 1$ ) not only reduces the maximum error but also the size of the large-error regions. It is also noted that this error reduction is consistent with the improvement in the grid size ratio as displayed in Figure 10. Acute grid line angles are also alleviated in the large-error regions as demonstrated in Figure 8. Similar improvements are also found in the other velocity component. In Table I the

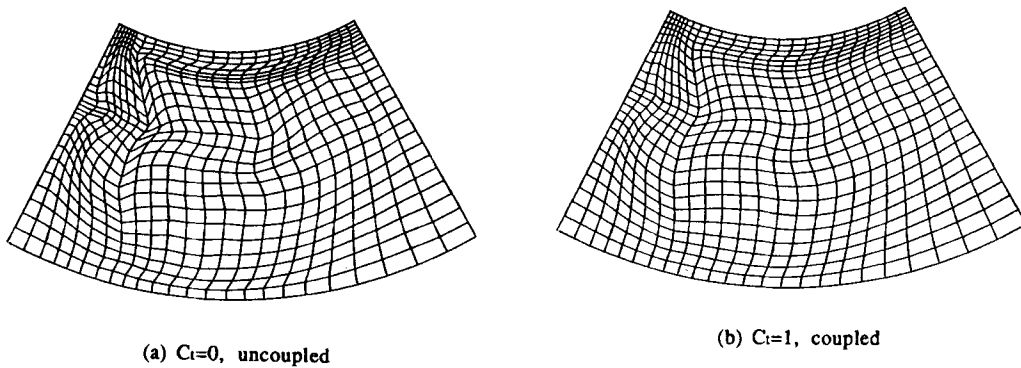


Figure 8. Adaptive grid lay-outs

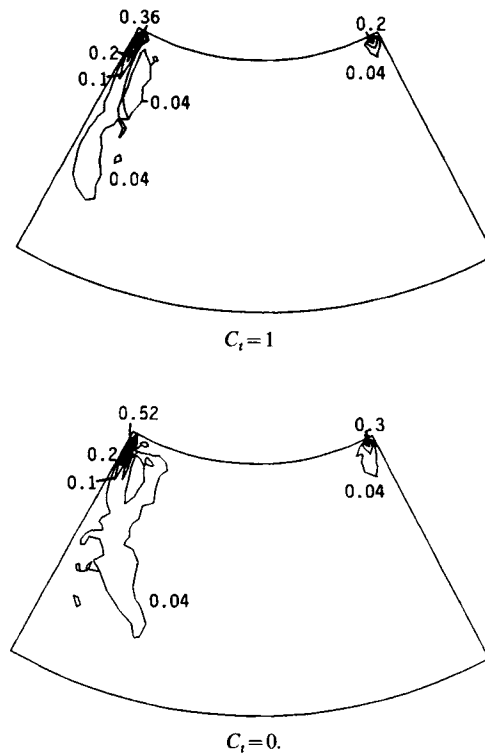


Figure 9. Solution error distributions for radial velocity component

solutions obtained with the various grids are summarized. By using the modified method (25-A), about 40% improvement in accuracy over the original method (25-AU) is achieved. Also note that the modified method with  $25 \times 25$  base grid yields the same accuracy as the  $41 \times 41$  uniform grid solution. A numerical efficiency (ratio of CPU times) of a factor of five to six is obtained in the current problem.

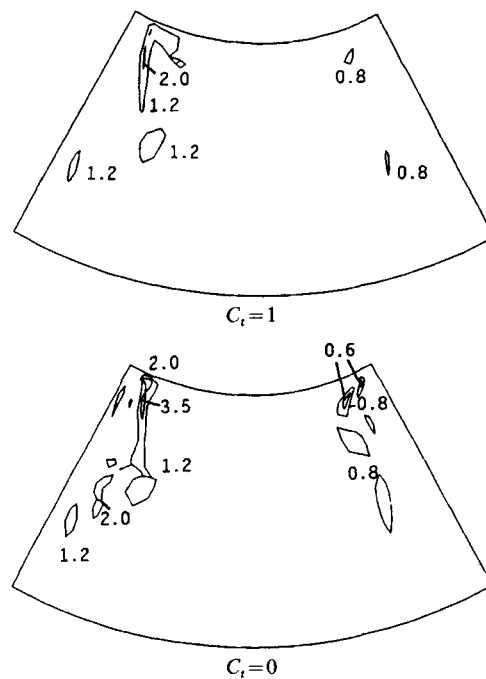


Figure 10. Grid size ratio contours

Table I. Summary of performance of different grids for polar cavity flow

Case	ERR	ERR <sub>MAX</sub>	CPU (VAX8600)	Total grid points
25-U	32.6	96.6	131	625
25-A	10.7	38.1	151	625
25-AU	14.8	55.7	171	625
41-U	11.8	35.9	795	1681
61-U	5.2	16.1	3580	3721
81-U	3.1	10.0	32900	6561
129-U	—	—	499562	16641

U, uniform grid; A, adaptive grid, coupled; AU, adaptive grid, uncoupled.

$$\text{ERR} = \frac{1}{N} \sum_{i=1}^N \left( \frac{\sqrt{[(u-u_0)^2 + (v-v_0)^2]}}{\sqrt{(u_0^2 + v_0^2)}} \right)_i \times 100\%,$$

$$\text{ERR}_{\text{MAX}} = \text{Max}_{i=1}^N \left( \frac{\sqrt{[(u-u_0)^2 + (v-v_0)^2]}}{\sqrt{(u_0^2 + v_0^2)}} \right)_i \times 100\%,$$

where  $u$  and  $v$  are the coarse grid velocities,  $u_0$  and  $v_0$  are the  $129 \times 129$  fine grid velocities and  $N$  is the number of grid points.

#### 4.2. Backward-facing step flow

The second test problem for two-dimensional computation is a laminar backward-facing step flow with  $Re = 800$ . The definition of the Reynolds number is based on two-thirds of the maximum inlet velocity and twice the inlet height. The step height is 0.475 and the total channel height is 0.975. A parabolic inlet velocity is assumed. The base grid used is  $25 \times 25$  and a  $101 \times 101$

uniform fine grid solution is used as the reference solution for comparisons. In Figure 11 the adaptive grids are shown. Note that the length in the  $y$ -direction is scaled up by a factor of two to demonstrate the grids more clearly. Figure 12 compares the errors of the two adaptive solutions. In another study<sup>9</sup> we discussed the effects of the grid size ratio  $r$  and the grid line angle  $\theta$  on the truncation errors and concluded that sudden changes in the grid size (i.e.  $r$  deviates significantly from unity) and severely acute angles should be avoided. The modified method is found to improve both of these factors. Figure 13 demonstrates the improvement in the grid size ratio in

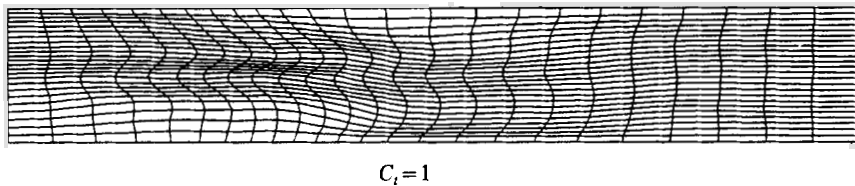
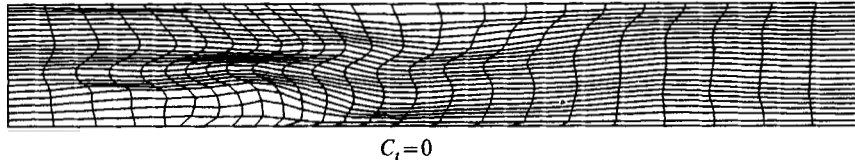


Figure 11. Adaptive grid lay-outs for backward-facing step

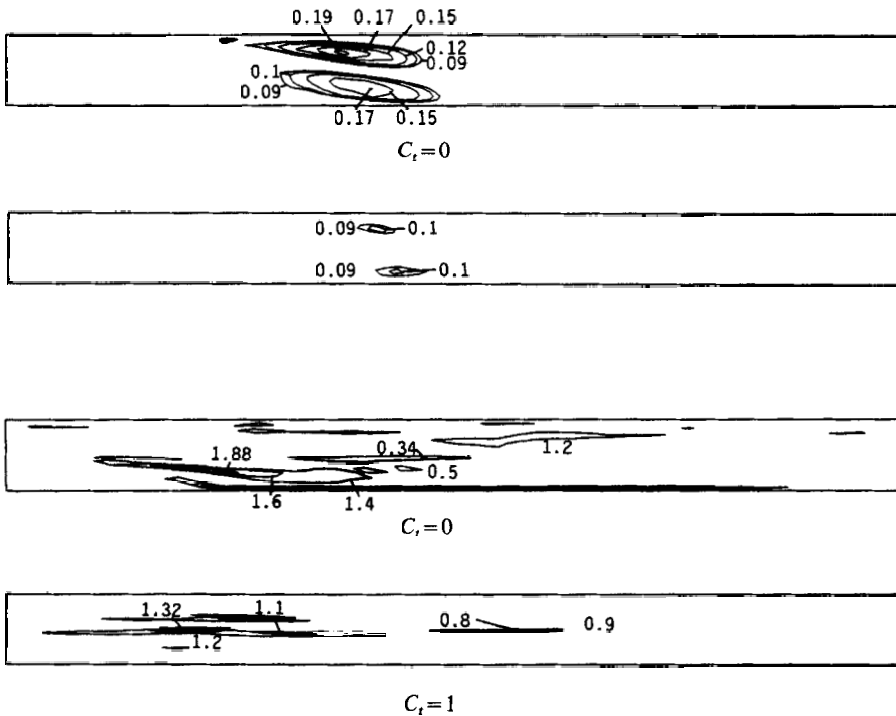


Figure 13. Distributions of grid size ratio

the large-error regions. With the coupled weight function the grid size ratios are limited to between 0.8 and 1.32, in contrast to a range from 0.34 to 1.88 with the uncoupled weight function. The grid line angles are also generally smoother with the modified method, as is shown in Figures 11 and 14. The above findings may partially explain why the modified method improves the solutions. The usefulness of the method can be seen in Table II. In the table,  $x_1/s$  is the size of the corner bubble, where  $s$  is the step height. The accuracy achieved by the current method is comparable to that of the  $41 \times 41$  uniform fine grid solution. The solution improvement over that of the original method (case 25-AU) is also obvious, particularly with respect to the prediction of the corner bubble size. The numerical efficiency in this case is roughly a factor of six. Note that the experimental value of  $x_1/s$  of Armaly *et al.*<sup>21</sup> was 14.0 and Guj and Stella<sup>22</sup> predicted a value of 12 with a grid number of  $41 \times 101$ .

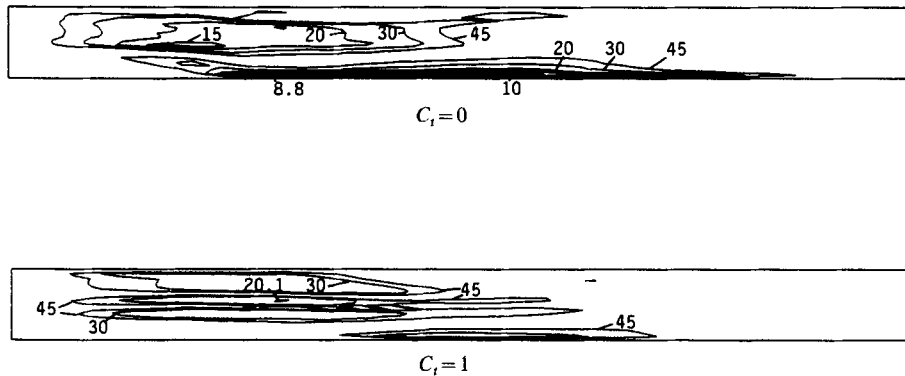


Figure 14. Distributions of grid line angles

Table II. Summary of performance of different grids for backward-facing step flow

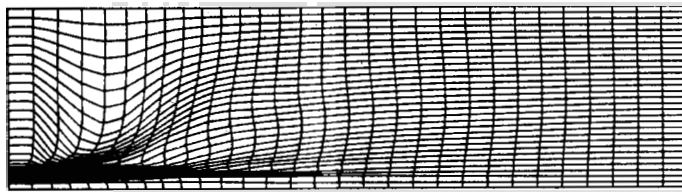
Case	$x_1/s$	ERR	ERR <sub>MAX</sub>	CPU (VAX8600)	Total grid points
25-U	9.5	14.5	49.6	682	625
25-A	11.8	3.5	15.3	720	625
25-AU	10.6	5.5	19.1	751	625
41-U	10.6	5.6	18.1	4551	1681
61-U	11.7	2.4	8.0	15612	3721
81-U	11.8	1.4	4.5	85445	6561
101-U	12.0	—	—	321721	10201

U, uniform grid; A, adaptive grid, coupled; AU, adaptive grid, uncoupled.

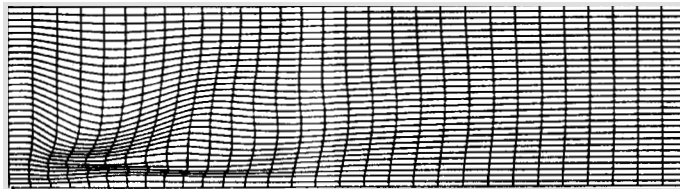
$$\text{ERR} = \frac{1}{N} \sum_{i=1}^N \left( \frac{\sqrt{[(u-u_0)^2 + (v-v_0)^2]}}{\sqrt{(u_0^2 + v_0^2)}} \right)_i \times 100\%,$$

$$\text{ERR}_{\text{MAX}} = \text{Max}_{i=1}^N \left( \frac{\sqrt{[(u-u_0)^2 + (v-v_0)^2]}}{\sqrt{(u_0^2 + v_0^2)}} \right)_i \times 100\%,$$

where  $u$  and  $v$  are the coarse grid velocities,  $u_0$  and  $v_0$  are the  $101 \times 101$  fine grid velocities and  $N$  is the number of grid points.



(a)  $C_t=0$ ,  $R=0.1$ ,  $31 \times 31$



(b)  $C_t=1$ ,  $R=0.1$ ,  $31 \times 31$

Figure 15. Adaptive grid arrangements

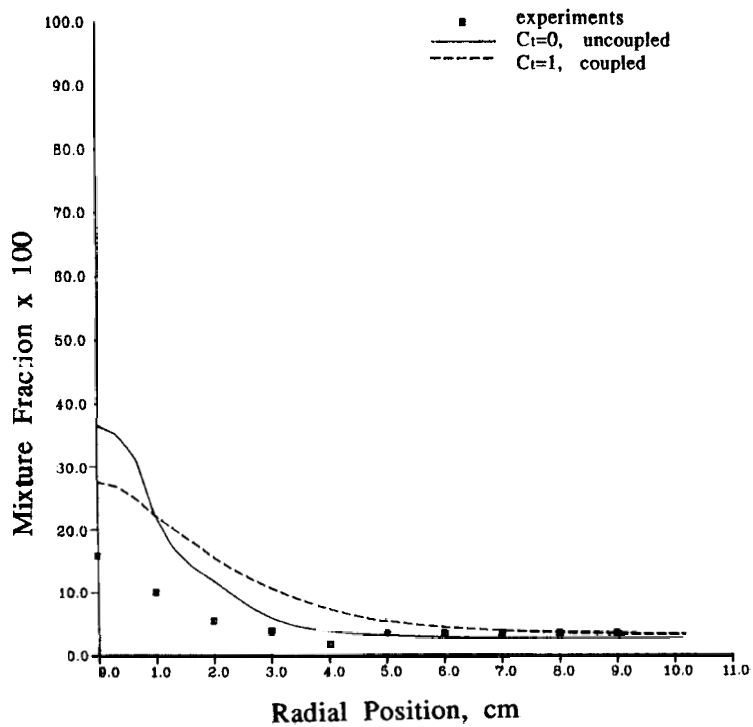


Figure 16. Comparison of radial profiles of mixture fraction at  $x = 32.7$ ;  $31 \times 31$ ,  $R = 0.1$

#### 4.3. Reacting sudden expansion pipe flow

The last test case is a turbulent reacting sudden expansion pipe flow. A standard  $K-\epsilon$  turbulence model and the fast chemistry combustion model<sup>23</sup> are employed. The specifications of the dimensions and boundary conditions of this problem can be found in Reference 24. The adaptive grid arrangements are shown in Figure 15. Again, this figure reveals that a better grid is obtained with the coupled weight function. Both the grid size variation and the grid line angle are smoother. Note that a trace of the flame front can be seen in the grid distribution even before the final calculation is conducted. A typical comparison of the solutions using the two approaches is shown in Figure 16. In this figure the radial profiles of the mixture fraction are demonstrated. Although the modified method yields only a slightly better solution in this case, it is found that if larger  $R$  (i.e. stronger grid adaption) is used, the solution with the uncoupled weight function diverges. In Figure 17 the adaptive solutions with the coupled weight function and  $R=0.25$  are compared with the uniform grid solutions. It is seen that the adaptive solutions are much closer to the experimental data near the axis.

In a turbulent reacting flow it may be inappropriate to attribute the solution improvement solely to the numerical error reduction, since the situation is further complicated by the adequacy of the physical methods of turbulence and combustion. Nevertheless, in this test case the modified method did provide a smoother grid which yielded a converged and improved solution. It should be noted that, for a complex flow problem, redistribution of the grid alone may not always improve the solution accuracy, since with a fixed number of grid points there is a limit on the

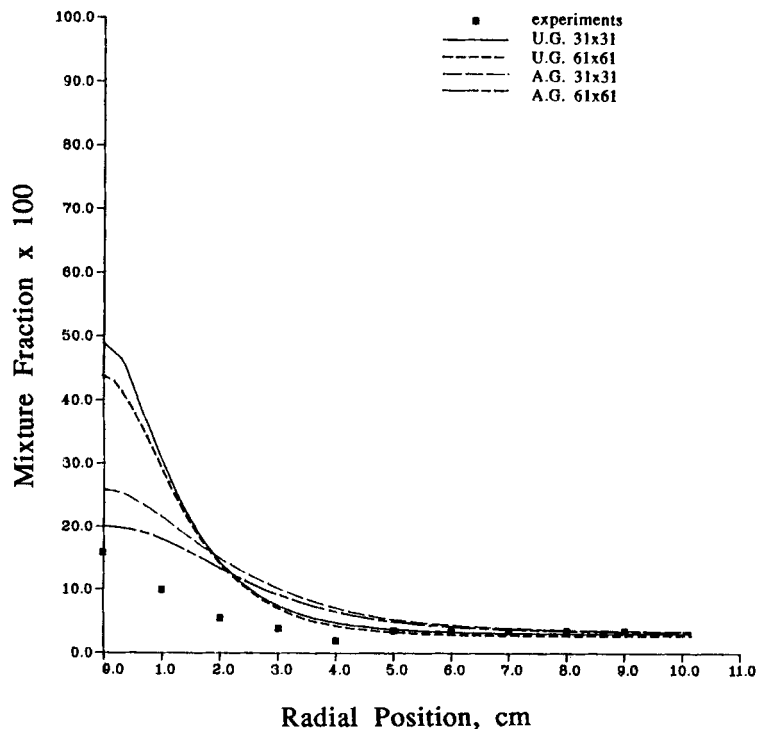


Figure 17. Comparison of radial profiles of mixture fraction at  $x=32.7$ ;  $R=0.25$  (U.G., uniform grid, A.G., adaptive grid)

solution accuracy. In this situation, use of a local refinement method together with the moving grid method can be a better approach.<sup>14</sup>

According to another study by the authors,<sup>9</sup> a large truncation error in the convection terms arises from improper grid size, severe non-uniformity of the grid (large  $r$ ), improper grid line angle as well as large values of the derivatives of flow properties. Therefore a possible error reduction can be achieved by improving these factors. Since the moving grid method provides a better resolution in high-gradient regions and the adaptive grid also tends to align with local streamlines, these can result in an error reduction.<sup>9</sup> The present modified method is shown to improve the grid size ratio and the grid line angle as demonstrated in the test cases. The statistics of the results indicates that the grid improvement due to the modified method yields a further error reduction and a better solution.

## 5. CONCLUSIONS

In the present study, one-dimensional model equations and two-dimensional flow problems have been employed to demonstrate the usefulness of a modified moving grid method. It is concluded that with a fixed number of grid points the present modified method can further improve the solution by using a coupled weight function. A major contribution of the modification is probably due to the improvement in the grid uniformity as well as the grid smoothness. The present method can be conveniently applied to three-dimensional problems.

## REFERENCES

1. D. A. Anderson, 'Adaptive grid methods for partial differential equations', in K. Ghia and U. Ghia (eds), *Advances in Grid Generation, FED-5*, ASME, New York, 1983.
2. H. A. Dwyer, R. J. Kee and B. R. Sanders, 'An adaptive grid method for problems in fluid mechanics and heat transfer', *AIAA J.*, **18**, 1205-1212 (1980).
3. H. A. Dwyer, 'Grid adaption for problems in fluid dynamics', *AIAA J.*, **22**, 1705-1712 (1984).
4. W. Shyy, 'Computation of complex fluid flows using an adaptive grid method', *Int. j. numer. methods fluids*, **8**, 475-489 (1988).
5. A. T. Hsu, 'The effect of adaptive grid on hypersonic nozzle flow calculations', *AIAA Paper 89-0006*, 1989.
6. M. J. Berger and J. Olinger, 'Adaptive mesh refinement for hyperbolic partial differential equations', *J. Comput. Phys.*, **53**, 484-512 (1984).
7. S. C. Caruso, J. H. Ferziger and J. Olinger, 'Adaptive grid techniques for elliptic fluid flow problems', *AIAA Paper 86-0498*, 1986.
8. G. W. Hedstrom and G. H. Rodrigue, 'Adaptive grid methods for time-dependent partial differential equation', in *Multigrid Method, Lecture Notes in Mathematics 960*, Springer, Berlin, 1982, pp. 474-484.
9. D. Lee and Y. M. Tsuei, 'A formula for estimation of truncation error of convection terms in a curvilinear coordinate system', *J. Comput. Phys.*, in press.
10. J. F. Thompson, Z. U. A. Warsi and C. W. Mastin, *Numerical Grid Generation*, North-Holland, Amsterdam, 1985.
11. D. A. Anderson, J. C. Tannehill and R. H. Pletcher, *Computational Fluid Mechanics and Heat Transfer*, McGraw-Hill, New York, 1984, Chap. 10.
12. D. Lee and W. Shyy, 'A study of one-dimensional transport problem with strong convection and source terms', *General Electric Technical Report 86CRD184*, 1986; also *Proc. 18th Ann. Pittsburgh Conf.*, School of Engineering, University of Pittsburgh, Pittsburgh 1987, pp. 1845-1851.
13. H. J. Crowder and C. Dalton, 'Errors in the use of nonuniform mesh systems', *J. Comput. Phys.*, **7**, 32-45 (1971).
14. D. Lee and Y. M. Tsuei, 'A hybrid adaptive gridding procedure for the recirculating fluid flow problems', submitted to *J. Comput. Phys.*
15. R. I. Kreis and H. A. Hassan, 'Application of a variational method for generating adaptive grids', *AIAA J.*, **24**, 404-410 (1986).
16. M. M. Rai and D. A. Anderson, 'Grid evolution in time asymptotic problems', *Numerical Grid Generation Techniques, NASA Conf. Publ. 2166*, 1980, pp. 409-430.
17. M. M. Rai and D. A. Anderson, 'Application of adaptive grids to fluid-flow problems with asymptotic solutions', *AIAA J.*, **20**, 496-502 (1982).
18. K. Nakahashi and G. S. Deiwert, 'Three-dimensional adaptive grid method', *AIAA J.*, **24**, 948-954 (1986).
19. L. Fuchs and N. Tillmark, 'Numerical and experimental study of driven flow in a polar cavity', *Int. j. numer. methods fluids*, **5**, 311-329 (1985).



20. D. Lee and H. T. Lee, 'Moving grid method for the computation of recirculating flow', *Proc. 5th Natl Conf. of the Chinese Society of Mechanical Engineering*, Chinese Society of Mechanical Engineering Taipei, Taiwan, 1988, pp. 43–50.
21. B. F. Armaly, F. Durst, J. C. F. Pereira and B. Schonung, 'Experimental and theoretical investigation of backward-facing step flow', *J. Fluid Mech.*, **127**, 473–496 (1983).
22. G. Guj and F. Stella, 'Numerical solution of high-*Re* recirculating flows in vorticity–velocity form', *Int. j. numer. methods fluids*, **8**, 404–416 (1988).
23. D. Lee, C. L. Yeh, Y. M. Tsuei, W. T. Jiang and Y. L. Chung, 'Numerical simulations of gas turbine combustor flows', *AIAA Paper 90-2305*, 1990.
24. M. H. Lewis and L. D. Smoot, 'Turbulent gaseous combustion, Part I: Local species concentration measurements', *Combust. Flame*, **42**, 183–196 (1981).